

MODELING THE LONGITUDINAL WALL IMPEDANCE INSTABILITY IN HEAVY ION BEAMS USING AN R-Z PIC CODE†

D. A. CALLAHAN, A. B. LANGDON, A. FRIEDMAN and D. P. GROTE

Lawrence Livermore National Laboratory, Livermore CA 94550 and

I. HABER

U.S. Naval Research Laboratory, Washington DC 20375.

(Received 3 December 1990)

The effects of the longitudinal wall impedance instability in a heavy ion beam are of great interest for heavy ion fusion drivers. We are studying this instability using the R-Z thread of the WARP PIC code.¹ We describe the code and our model of the impedance due to the accelerating modules of the induction linac as a resistive wall. We present computer simulations that illustrate this instability.

1 INTRODUCTION

The longitudinal wall impedance instability occurs when a beam travels down a pipe with finite impedance. This instability may have a significant effect on accelerated beams for heavy ion fusion applications since final focusing places requirements on the beam quality. In order to study this instability, we have written an RZ particle-in-cell code. This code is part of the WARP family of codes.¹ It is an electrostatic, $2\frac{1}{2}$ -dimensional PIC code. The simulation is done in a window that moves with the beam velocity and has periodic boundaries in the axial direction. Since our beams are not neutral, we add a linear focusing force, which keeps the beam radially confined and mocks up the A-G focusing used in experiments.

2 LINEAR THEORY

We can calculate a dispersion relation for a beam in a pipe with a resistive wall using fluid equations for the velocity, u , and the line charge density, λ . The dynamics of a

† Work performed in part under the auspices of the U.S. Department of Energy by Lawrence Livermore National Laboratory under contract W-7405-ENG-48.

cold beam are described by:

$$\frac{\partial \lambda}{\partial t} + \frac{\partial(\lambda u)}{\partial z} = 0 \quad (1)$$

$$\frac{\partial u}{\partial t} + u \frac{\partial u}{\partial z} = \frac{Ze}{M} E_z. \quad (2)$$

We linearize with $u = \tilde{u}$ in the beam frame, and $\lambda = \lambda_0 + \tilde{\lambda}$. In the limit that the wavelength for perturbations is long compared with the pipe radius, the perturbed electric field is given by

$$\tilde{E}_z = -g \frac{\partial \tilde{\lambda}}{\partial z} - \eta \delta I_b, \quad (3)$$

where $g = -\ln(a/b)/2\pi\epsilon_0$ in MKS units, a is the beam radius, b is the wall radius, and η is the resistance per unit length. The perturbed beam current is given by $\delta I_b = v_b \tilde{\lambda} + \lambda_0 \tilde{u}$, where v_b is the beam velocity. If we let $\tilde{\lambda}, \tilde{u} \sim e^{i(kz - \omega t)}$, we find the dispersion relation in the beam frame,

$$0 = 1 - \frac{k^2 v_p^2}{\omega^2} + i \frac{\eta v_p^2 (kv_b + \omega)}{g \omega^2}, \quad (4)$$

where $v_p^2 = Zeg\lambda_0/M$. If we assume $v_b \gg \omega/k$ and $\eta v_b/gk \ll 1$ then, the dispersion relation can be rewritten as

$$\frac{\omega}{kv_p} = \pm \sqrt{1 - i\eta v_b/gk} \approx (1 - i\eta v_b/2gk) \quad (5)$$

The real part of this equation gives a wave traveling with the phase velocity, $\omega_{\text{real}}/k = \pm v_p$. The forward-traveling wave ($\omega_{\text{real}} = +kv_p$) damps with decay rate $\omega_i = -\eta v_b v_p/2g$, while the backward-traveling wave ($\omega_{\text{real}} = -kv_p$) grows with growth rate $\omega_i = +\eta v_b v_p/2g$. For long-wavelength perturbations, we expect to see forward traveling waves damp and backward-traveling waves grow independent of wavelength.

3 MODEL OF THE RESISTIVE WALL

We wish to explore this instability with our PIC code. First, we must develop a model for the resistive wall in the code. We would like to formulate a scheme that includes the resistive wall in the calculations without explicitly using the beam current. We want to avoid estimating the current through z cross sections, that is, using a highly localized current. Involving the Poisson solution lets us, in effect, estimate a current as some weighted average over a volume of pipe of length \sim beam radius. We hope that this model will be more-physical and smoother.

We begin with a continuity equation for the wall surface charge, σ , which has units of charge/area:

$$\frac{\partial \sigma}{\partial t} + \frac{\partial K_z}{\partial z} = 0, \quad (6)$$

where K_z is the surface current. We also have Ohm's law, $2\pi b\eta K_z = E_z$, where η is the resistance per unit length. Plugging this into the continuity equation yields

$$\frac{\partial \sigma}{\partial t} = -\frac{\partial}{\partial z} \left(\frac{E_z}{2\pi b\eta} \right). \quad (7)$$

Integrating this equation over the surface and assuming cylindrical symmetry gives

$$\frac{\partial}{\partial t} \int_{z_1}^{z_2} \sigma dz = -\frac{1}{2\pi b\eta} [E_z(z_2) - E_z(z_1)], \quad (8)$$

where we have taken the limits on z to be z_1 to z_2 . We define the electrostatic potential, ϕ , by

$$E_z(z') = -\left. \frac{\partial \phi}{\partial z} \right|_{z'}. \quad (9)$$

Consider the case of $z_2 = z_1 + \Delta z$ where Δz is small. Over this range, we can assume that σ doesn't change much, and we can evaluate the integral over σ , giving us

$$\frac{\partial}{\partial t} \int_{z_1}^{z_1 + \Delta z} \sigma dz = \Delta z \frac{\partial \sigma}{\partial t}. \quad (10)$$

Defining the surface charge, sQ , as ${}^sQ = 2\pi b\Delta z\sigma$, and using the results of Equations (9) and (10) in Equation (8), gives

$$\frac{\partial({}^sQ)}{\partial t} = \frac{1}{\eta} \left[\left. \frac{\partial \phi}{\partial z} \right|_{z_1 + \Delta z} - \left. \frac{\partial \phi}{\partial z} \right|_{z_1} \right]. \quad (11)$$

Since we have assumed that Δz is small, we can expand $\partial\phi/\partial z$ in a Taylor series. Taking the first two terms of this expansion and substituting into Equation (11) gives the result:

$$\frac{\partial({}^sQ)}{\partial t} = \frac{\Delta z}{\eta} \frac{\partial^2 \phi}{\partial z^2}. \quad (12)$$

This equation is then solved simultaneously with Poisson's equation in the code.

The solve is done by Fourier-transforming Equation (12) with respect to z and then using a finite-difference approximation to the time derivative. Doing this gives

$${}^s\tilde{Q}^{n+1} = {}^s\tilde{Q}^n - \frac{\Delta t \Delta z}{\eta} k^2 \tilde{\phi}^{n+1}, \quad (13)$$

where the superscript denotes the time level and the tilde denotes the Fourier transform. We can write Poisson's equation as

$$(\nabla_r^2 - k^2)\tilde{\phi}^{n+1} = -\frac{\tilde{\rho}^{n+1}}{\epsilon_0} \quad (14)$$

where ∇_r^2 is the radial part of ∇^2 . At the wall, $\tilde{\rho}^{n+1}$ is composed of the charge density due to the plasma plus the charge density due to the surface charge, ${}^s\tilde{Q}^{n+1}$. We substitute for ${}^s\tilde{Q}^{n+1}$ in Poisson's equation at the wall from Equation (13) and are left with an equation for $\tilde{\phi}^{n+1}$ in terms of the surface charge at the last time step, ${}^s\tilde{Q}^n$, and the plasma density. The radial part of the Laplacian is differenced to give a tridiagonal system of equations for each value of k . These systems are solved via Gaussian elimination using the boundary condition $\tilde{\phi} = 0$ for $r > r_{\text{wall}}$ to give $\tilde{\phi}^{n+1}$. We then update the surface charge using Equation (13) to complete the field solution.

We would like to connect our model with the simpler model used in the linear analysis in the long-wavelength limit. Rewrite Equation (12) in terms of the electric field and the surface charge density and then Fourier transform in space and time:

$$-\omega 2\pi b\sigma = -kE_z/\eta. \quad (15)$$

In the long-wavelength limit, the line charge density can be written as $\lambda \approx -2\pi b\sigma$, and in the lab frame $\omega \approx kv_b$, so that

$$E_z = -\eta v_b \lambda, \quad (16)$$

or, in terms of the beam current, $I_b = v_b \lambda$,

$$E_z = -\eta I_b, \quad (17)$$

which is the contribution to the electric field that we used in the linear analysis in Equation (3). So, our model does reduce to the simple model used in the linear theory in the long-wavelength limit.

4 SIMULATIONS

We present two simulations: a traveling wave moving backward and a traveling wave moving forward. If we Fourier-transform the linearized continuity equation, we see that

$$\frac{\tilde{\lambda}}{\lambda_0} = \frac{k\tilde{u}}{\omega}, \quad (18)$$

where $\tilde{\lambda}$ and \tilde{u} are the perturbed quantities. This tells us that for a forward-traveling wave, ($\omega = +kv_p$), the relationship between the perturbation in velocity and the perturbation in line charge is

$$\frac{\tilde{\lambda}}{\lambda_0} = +\frac{\tilde{u}}{v_p}, \quad (19)$$

TABLE 1
Simulation Parameters

Radius of beam, $a = 2.33568 \times 10^{-02}$ m
Radius of the wall, $b = 5.0 \times 10^{-02}$ m
Beam velocity, $v_b = 1.0 \times 10^{07}$ m/s
Wall resistivity, $\eta = 500 \Omega/\text{m}$
Line charge density, $\lambda = 1.46 \times 10^{-05}$ C/m
Beam current, $I = 146.9$ Amps
Phase velocity, $v_p = 1.26 \times 10^{06}$ m/s
Thermal velocity, $v_{th,z} = 1.65 \times 10^{04}$ m/s
Number of gridpoints in r , $N_r = 64$
Number of gridpoints in z , $N_z = 128$
Number of simulations particles = 4.062×10^{04}
Number of real particles, $N_p = 1.094 \times 10^{14}$
Mass of particle, $M = 12$ amu
$g = \ln(b/a)/(2\pi\epsilon_0) = 1.368 \times 10^{10}$
$\eta v_b/gk = 6.98 \times 10^{-02} < 1$

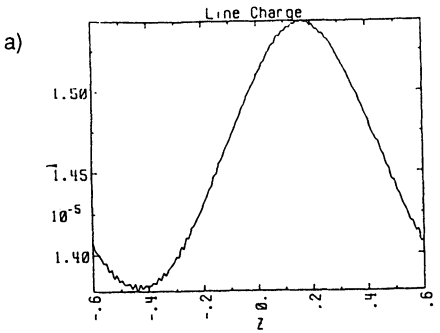
while for a backward-traveling wave, ($\omega = -kv_p$), the relationship is

$$\frac{\tilde{\lambda}}{\lambda_0} = -\frac{\tilde{u}}{v_p}. \quad (20)$$

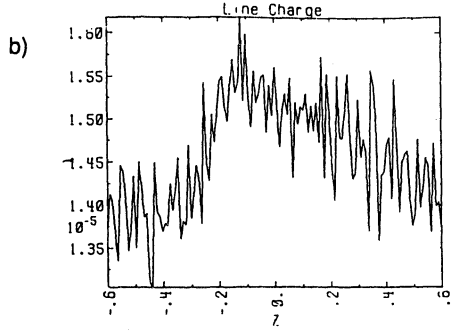
We add a sinusoidal perturbation with wavelength equal to the length of the window (1.2 meters) to the line charge density and the velocity, using the relationships in Equations (19) and (20). This perturbation is 5% of the line charge density and 5% of the phase velocity, v_p . The beam is infinite in length and travels to the right in the figures. The relevant simulation parameters are summarized in Table 1.

The backward wave simulation is shown in Figures 1a–1f. The perturbation does not remain sinusoidal; instead, it steepens and becomes more localized. This may suggest that our initial condition is not a pure traveling wave. After $4 \mu\text{s}$, the beginnings of a second bump in the line charge are visible (see Figure 1c). As time progresses, both perturbations grow (Figures 1d–1f). The perturbation travels to the left (backward with respect to the beam) and is returned via the periodic boundary conditions on the right side of the simulation region. The general shape of the growing perturbation is similar to the results of Bisognano *et al.*² in their studies of longitudinal waves on a beam in 1-d.

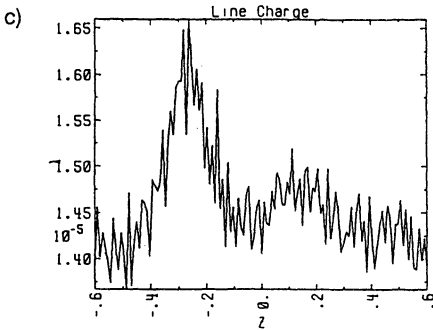
The forward wave simulation is shown in Figures 2a–2f. Again, the perturbation does not remain sinusoidal; it, too, steepens and becomes localized. However, if we compare Figure 2f (forward-traveling) with Figure 1f (backward-traveling), we do not see growth in the forward-traveling wave, nor do we see the appearance of the second bump in the line charge density as we saw in the backward-traveling-wave simulation. This qualitatively agrees with the results of the linear theory—the forward-moving wave does not grow, while the backward-moving wave does. We do not see the decay that is expected in the forward wave; we believe that the absence of the decay is due to the presence of some small component of backward-traveling wave in the initial conditions. We expect to be able to isolate these two cases more purely in the near future.



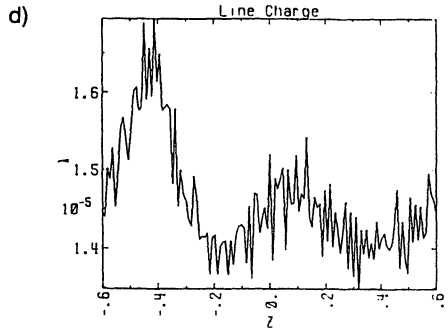
Step 0, $T = 0.0000 \mu\text{s}$, $Z_{\text{beam}} = 0.0000 \text{m}$
 Here beam with cylindrical load, etc - 599.
 Periodic E-Y uniform focusing, 6%128
 Debbie Callahan 11/27/98 28:03:44 PRC5



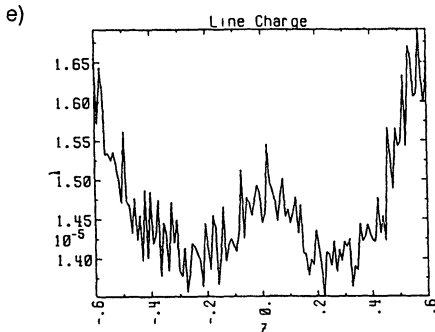
Step 1000, $T = 2.0000 \mu\text{s}$, $Z_{\text{beam}} = 20.0000 \text{m}$
 Here beam with cylindrical load, etc - 599.
 Periodic E-Y uniform focusing, 6%128
 Debbie Callahan 11/27/98 28:03:44 PRC5



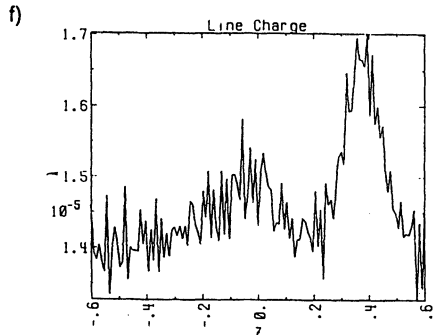
Step 2000, $T = 4.0000 \mu\text{s}$, $Z_{\text{beam}} = 40.0000 \text{m}$
 Here beam with cylindrical load, etc - 599.
 Periodic E-Y uniform focusing, 6%128
 Debbie Callahan 11/27/98 28:03:44 PRC5



Step 3000, $T = 6.0000 \mu\text{s}$, $Z_{\text{beam}} = 60.0000 \text{m}$
 Here beam with cylindrical load, etc - 599.
 Periodic E-Y uniform focusing, 6%128
 Debbie Callahan 11/27/98 28:03:44 PRC5



Step 4000, $T = 8.0000 \mu\text{s}$, $Z_{\text{beam}} = 80.0000 \text{m}$
 Here beam with cylindrical load, etc - 599.
 Periodic E-Y uniform focusing, 6%128
 Debbie Callahan 11/27/98 28:03:44 PRC5



Step 5000, $T = 10.0000 \mu\text{s}$, $Z_{\text{beam}} = 100.0000 \text{m}$
 Here beam with cylindrical load, etc - 599.
 Periodic E-Y uniform focusing, 6%128
 Debbie Callahan 11/27/98 28:03:44 PRC5

FIGURE 1a-f. Line Charge (C/m) vs axial position at various times for the backward-traveling wave.

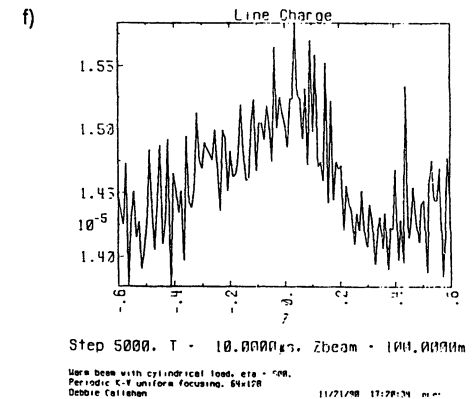
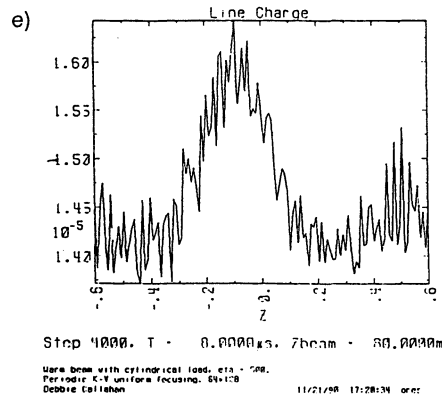
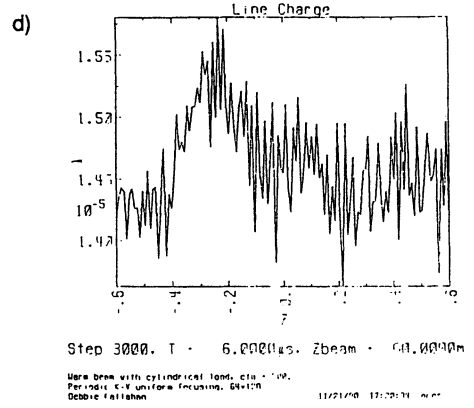
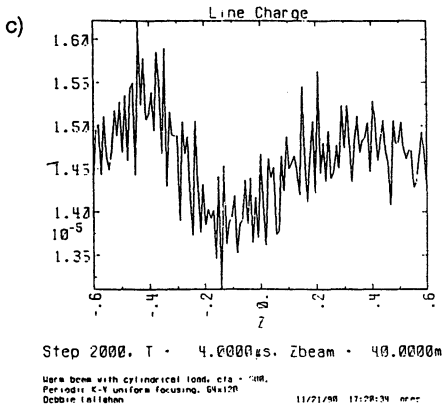
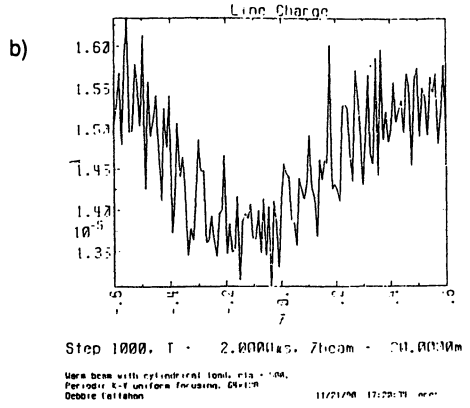
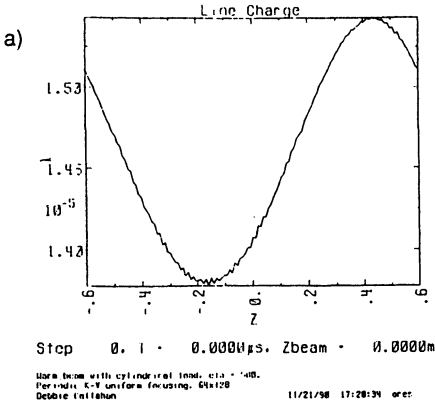


FIGURE 2a-f. Line Charge (C/m) vs axial position at various times for the forward-traveling wave.

5 CONCLUSIONS

We have derived and implemented a method for incorporating a resistive wall in our PIC code as a model of the impedance due to the accelerating modules of an induction linac. A simple linear theory predicts a growing wave traveling backward with respect to the beam velocity and a damped wave traveling forward. Our numerical model has shown this to be qualitatively true. Further study using this model will include effects of finite-length beams and a comparison of our model with other models³.

REFERENCES

1. A. Friedman, D. A. Callahan, D. P. Grote, A. B. Langdon, and I. Haber, in *Proceedings of the Conference on Computer Codes and the Linear Accelerator Community*, edited by R. K. Cooper and K. C. D. Chan (Los Alamos NM, 1990).
2. J. Bisognano, I. Haber, L. Smith, and A. Sternlieb, *IEEE Trans. Nucl. Sci.* **NS-28**, 3 (1981), p. 2513.
3. I. Hofmann and I. Bozsik, in *Proceedings of the Symposium on Accelerator Aspects of Heavy Ion Fusion*, (Darmstadt, Germany, 1982), Gesellschaft für Schwerionenforschung publication GSI-82-8, p. 181.